Supporting information

Cell-glucose gradients simulation with reaction-diffusion equations

To simulate the cell and glucose gradients throughout the chip, we propose a model of reaction-diffusion equations on a 1-dimensional spatial domain. This domain represents a linear section of the microfluidic chip. All simulations were performed with Matlab (R2014b version), using the pdepe package. In the equations, we define the cell density (u_1) and the glucose concentration (u_2). The equations reflect glucose consumption by the cells, and also the three states of behavior of the cells depending on the levels of glucose: growth, quiescence, and death.

The equations are as follows:

$$\frac{\partial u_1}{\partial t} = D_1 \frac{\partial^2 u_1}{\partial x^2} + \gamma(u_1,u_2) \quad (1)$$

$$\frac{\partial u_2}{\partial t} = D_2 \frac{\partial^2 u_2}{\partial x^2} - \beta \cdot u_1 \cdot u_2 \quad (2)$$

Initial conditions reflect the initial setting of the microfluidic chip, in which there is a constant concentration of glucose in the whole channel, and a constant density of cells in the whole channel except within the blood vessel. These conditions are reflected as follows:

$$u_1(0,x) = \begin{cases} u_1^0 & if\ x \in (L_1,L_{bv1}) \cup (L_{bv2},L_2) \\ 0 & otherwise \end{cases} \quad (3)$$

$$u_2(0,x) = \begin{cases} u_2^0 & if\ x \in (L_1,L_2) \\ 0 & otherwise \end{cases} \quad (4)$$

To consider the two scenarios of interest (i.e., presence and absence of diffusion ports), we use two different sets of boundary conditions. Cells are always considered to be unable to cross the boundaries of the microdevice. The right boundary is also considered always to be closed to glucose penetration. For the first simulation (absence of diffusion ports), the boundary conditions are defined simply as:

$$\frac{\partial u_1}{\partial x}(0,t) = \frac{\partial u_1}{\partial x}(L,t) = \frac{\partial u_2}{\partial x}(0,t) = \frac{\partial u_2}{\partial x}(L,t) = 0 \quad (5)$$

For the second scenario (presence of diffusion ports), we consider a mixed boundary condition that reflects the capacity of glucose to penetrate through the port. This is reflected in the equations as follows:

$$\frac{\partial u_1}{\partial x}(0,t) = \frac{\partial u_1}{\partial x}(L,t) = \frac{\partial u_2}{\partial x}(0,t) = 0 \quad (6)$$

$$\frac{\partial u_2}{\partial x}(L,t) + u_2^L = 0 \quad (7)$$

In the boundary conditions described above, the u_2^L term reflects the concentration of glucose outside the chip, that crosses through the port to create the expected gradient.

In equation (1), the term $\gamma(u_1,u_2)$ reflects the three scenarios to which cells may be subject: growth, quiescence, and death. This function is defined by parts, and responds to the following expression:

$$\gamma(u_1,u_2) = \begin{cases} \alpha \cdot u_1 & if\ u_2 > \gamma_{growth} \\ 0 & if\ u_2 \in [\gamma_{quiesc}, \gamma_{growth}) \\ -\delta \cdot u_1 \cdot u_2 & if\ u_2 < \gamma_{quiesc} \end{cases} \quad (8)$$

In the equations above, the symbols stand for the following meanings:

$u_1(x,t)$ - Cell population (cancer cells) along the 1-dimensional channel.

$u_2(x,t)$ - Glucose concentration along the 1-dimensional channel.

$D_1(x)$ - Cell diffusion rate.

$D_2(x)$ - Drug diffusion rate.

α - Cell replication rate (number of cell divisions per unit time).

β - Glucose consumption rate

δ - Cell death rate (in absence of glucose).

γ_{growth} - Glucose concentration threshold for cells to be in growth state.

γ_{quiesc} - Glucose concentration threshold for cells to be in quiescent state.

Table 1

Symbol	Meaning	Value	Source
u_1^0	Initial cell concentration (100.000 cells/u m)	1	Initial experimental conditions
u_2^0	Initial glucose concentration (per unit space)	50	Initial experimental conditions
D_1	Cell diffusion rate inside lumen (um/h)	0.001	Fitted to experimental results
D_2	Glucose diffusion rate inside lumen (um/h)	8.9	λm/s [https://bionumbers.hms.harvard.edu/bionumber.aspx?id=104089&ver=7]
α	Cell replication rate	0.05	As in [36]
β	Glucose consumption rate	0.8	Fitted to experimental results
δ	Cell death rate in absence of glucose	0.05	Fitted to experimental results
L_{bv1}	Blood-vessel (left side)	1/9	Initial experimental conditions
L_{bv2}	Blood-vessel (right side)	2/9	Initial experimental conditions

Table S1. Parameters used in the computational simulation.

Due to the absence of data on the concentration of glucose that induces quiescence and cell death, we adjusted these numbers to the behavior observed experimentally, in order to better reproduce cell behavior. To obtain simulation over time of the system described above, equations were solved numerically, with help of a finite difference method. The 24-hour time interval was divided into 150 time-steps. The 10 μm length space region was divided into 1000 small regions.

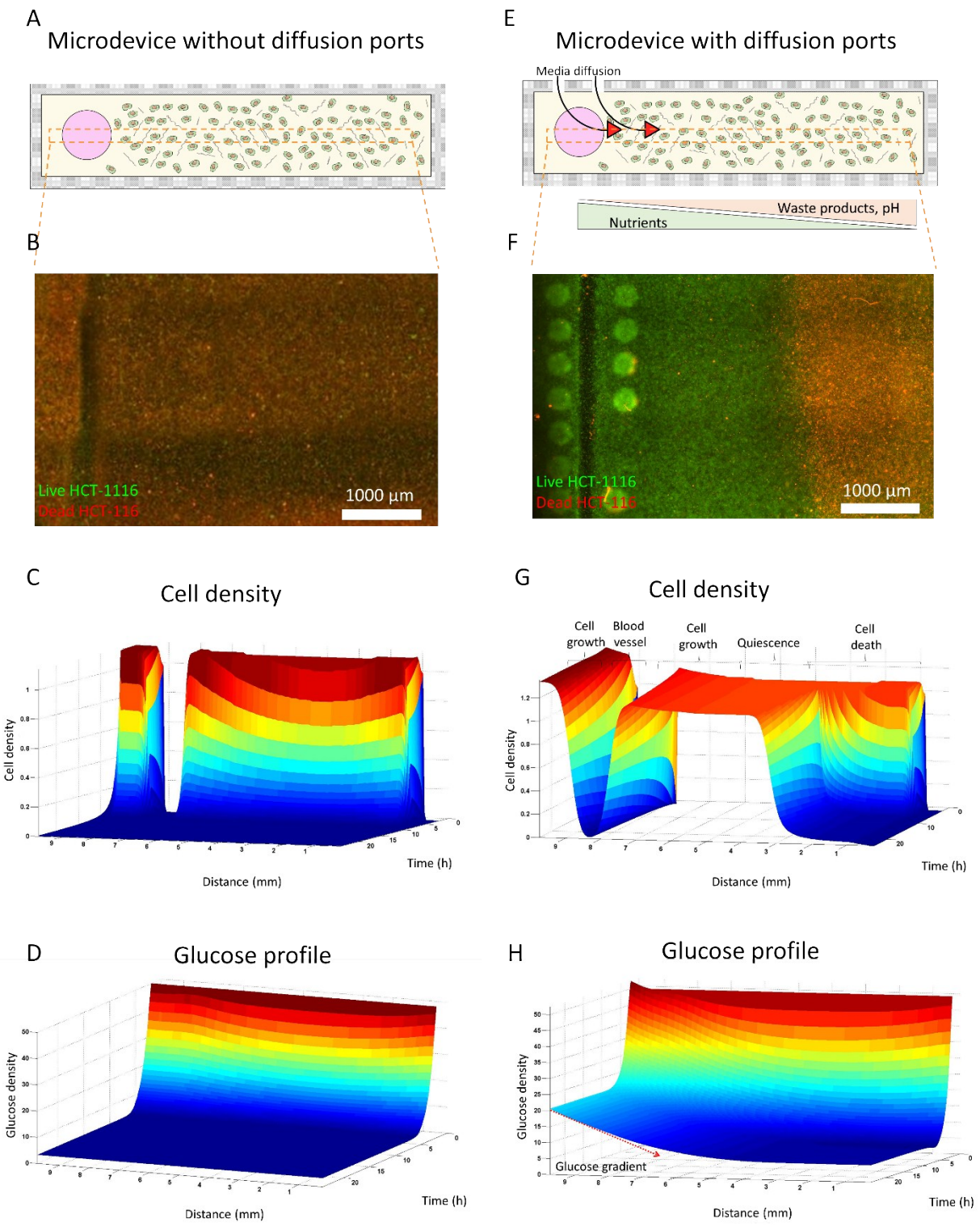

Supporting figure 1. Effect of diffusion ports. A) Scheme showing the initial design. The absence of diffusion ports on the top of the microdevice limited media diffusion inside the microdevice. B) Fluorescence microscopy image showing the intense necrosis in the absence of ports across the hydrogel. C-D) Computational simulation of the cell density and glucose profile across the hydrogel in the absence of diffusion ports. E) Scheme showing a microdevice including diffusion ports, which allowed media diffusion into the chamber. F) Fluorescence microscopy image showing the effect

of diffusion ports on cell viability. Media diffusion into the chamber led to the generation of two different regions, characterized by high cell viability and mortality respectively. G-H) Computational simulation of the cell density and glucose profile across the hydrogel in the presence of diffusion ports. The simulation shows the proliferative, quiescent, and necrotic area.

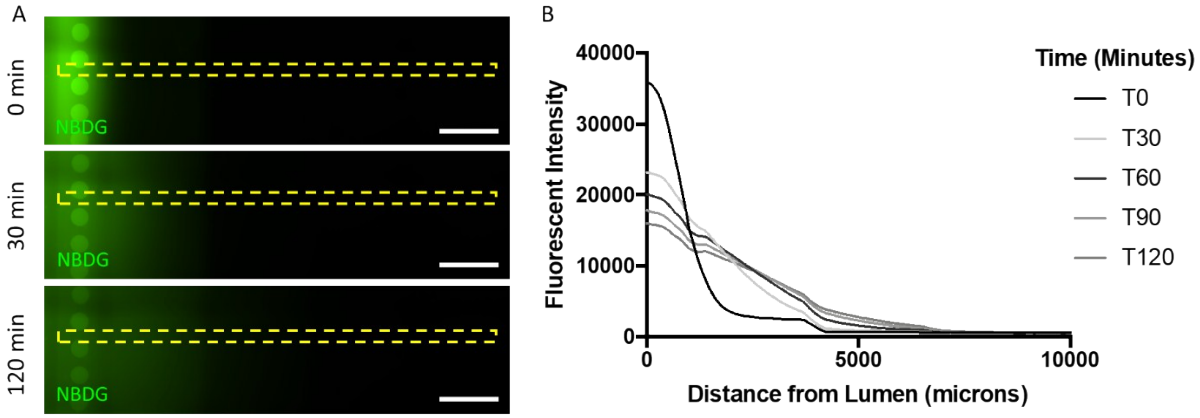

Supporting Figure 2. NBDG diffusion profile in the microdevice. A) The fluorescent glucose analog NBDG was dissolved in PBS at 200 µM and perfused through the central lumen. The NBDG diffusion profile across the collagen hydrogel was evaluated at different times. B) The graph shows the NBDG fluorescence profile across the yellow region. Given the large dimensions of the chamber (i.e., 1.5 cm length x 1.0 cm width), NBDG required a long time to reach the furthest regions from the lumen.

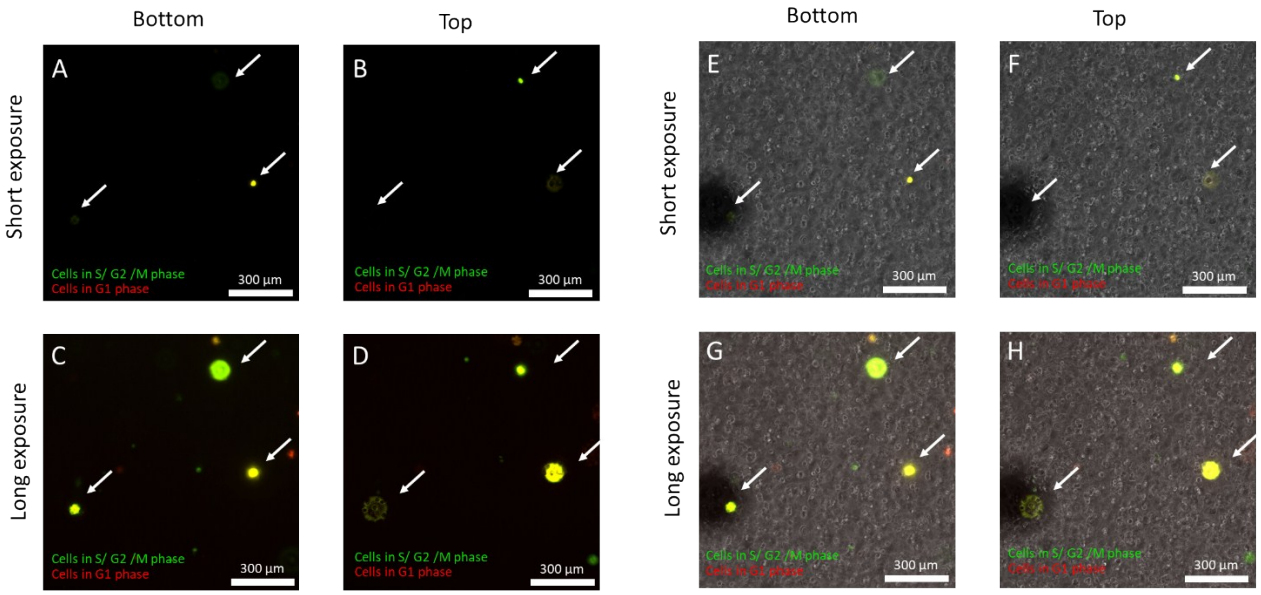

Supporting Figure 3. HCT-116 cells transfected with the FUCCI cell cycle sensor. A-B) Transfected cells were embedded in the hydrogel with non-transfected cells and Z-stacks were acquired using a short exposure time (50 ms). Images show the bottom (A) and top (B) of the stack. C-D) Same field of view acquired using long exposure (1000 ms). The images show a larger number of transfected cells and the brightest cells appear as larger spots. E-H) Same field of view showing the fluorescence images overlaid with the brightfield image.

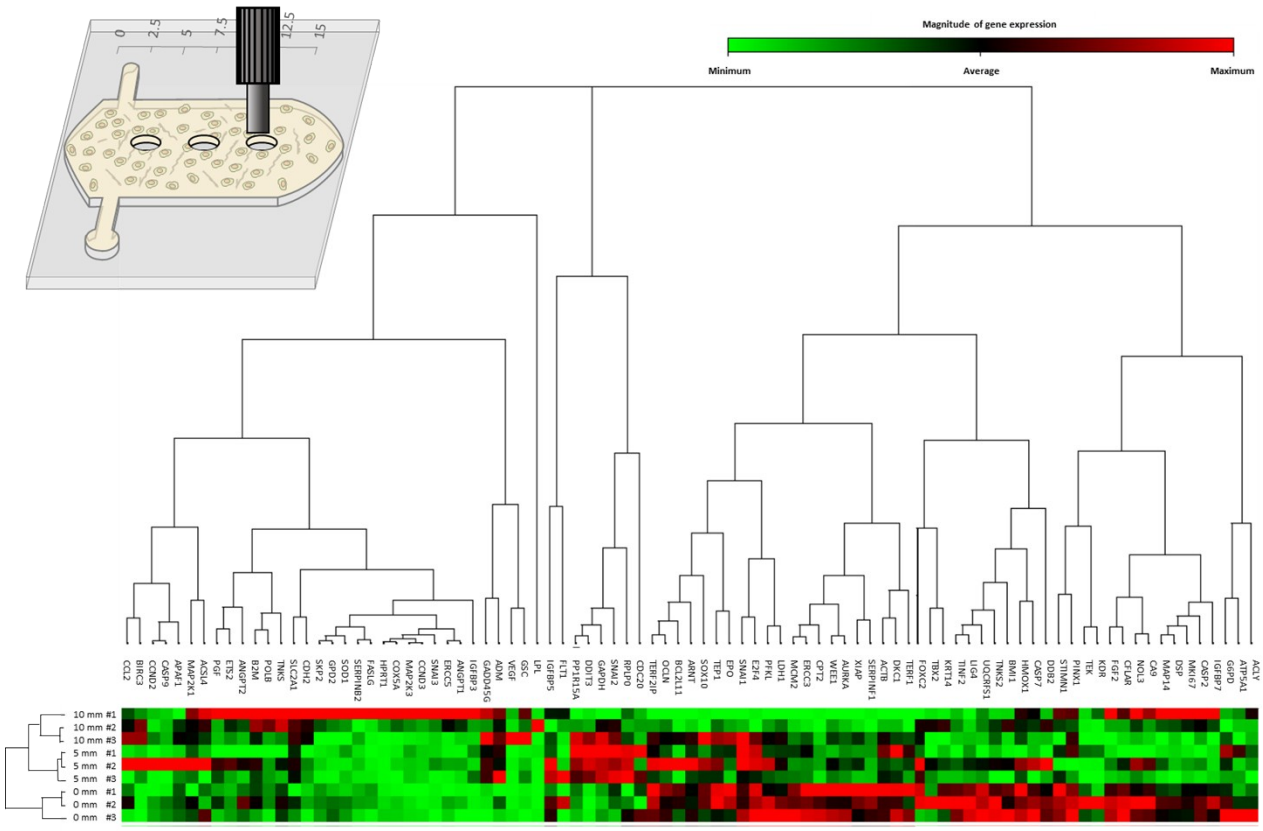

Supporting Figure 4. Gene profile analysis. HCT-116 cells were cultured at 5 million cells/ml in the microdevice. After 24 hours in culture, cells were isolated using a biopsy punch (1mm diameter) at different distances from the lumen (i.e., 0, 5 and 10 mm). The expression of ninety genes related with multiple pathways was analyzed and presented in a heat-map showing non-supervised hierarchical clustering of co-regulated genes.

Table 2			
Gene	**Full name**	**Function**	**State at 10mm from lumen**
IGFBP3	Insulin-like growth factor-binding protein 3	Binds to insulin-like growth factors (IGFs). In tissues, IGBP3 blocks IGF access to its receptor, decreasing cell proliferation.	Upregulated
GADD45G	Growth arrest and DNA damage inducible gamma	Involved in DNA repair and is upregulated after cellular stress.	Upregulated
BIRC3	Baculoviral IAP repeat containing 3	Apoptosis inhibition by binding to tumor necrosis factor-associated factors (TRAFs). BIRC3 blocks apoptosis due to deprivation of serum and growth factors.	Upregulated
ADM	Adrenomedullin	ADM induces angiogenesis, vasodilatation, and ROS resistance.	Upregulated
PINX1	PIN2 (TERF1) interacting telomerase inhibitor 1	Involved in telomere stability. PINX1 inhibits telomerase activity, therefore leading to telomere shortening and decrease genome stability and cell proliferation.	Downregulated
STMN1	Stathmin 1	Regulates cytoskeleton stability by promoting microtubule depolymerization.	Downregulated
FGF2	Fibroblast growth factor 2	Induces cell proliferation and angiogenesis.	Downregulated
DKC1	Dyskerin pseudouridine synthase 1	Stabilizes the telomerase complex therefore enabling continuous self-renewal.	Downregulated
BMI1	BMI1 proto-oncogene	Indispensable for self-renewal on both normal and cancer cells. Also involved in radiation-induced DNA damage repair. BMI1 absence leads to increase sensitivity to radiotherapy and double strand breaks.	Downregulated
UQCRFS1	Ubiquinol-cytochrome C reductase, rieske iron-sulfur polypeptide 1	Subunit of the complex III in the mitochondrial respiratory chain. It has been linked to increase in cancer aggressiveness.	Downregulated
TINF2	TERF1 interacting nuclear factor 2	Encodes a protein of the shelterin, a protein complex that protect the telomere from DNA damage.	Downregulated
DDB2	DNA damage-binding protein 2	DDB2 dimerizes with DDB1 in order to form the UV-damaged DNA-binding protein complex (the UV-DDB complex), which repairs UV-induced DNA damage.	Downregulated
TNKS2	Tankyrase-2	Involved in Wnt pathway, vesicle trafficking and telomere length and stability.	Downregulated
MCM2	Minichromosome maintenance complex component 2	Necessary for the initiation of cell replication.	Downregulated
WEE1	WEE1 G2 checkpoint kinase	Mitotic checkpoint. WEE1 prevents cells to entry in mitosis during substrate competition or DNA damage.	Downregulated
ERCC3	ERCC excision Repair 3, TFIIH core complex helicase subunit	Repairs DNA damage generated by radiation.	Downregulated
XIAP	X-linked inhibitor of apoptosis protein	Inhibitor of caspase 3, 7 and 9, blocking caspase-mediated apoptosis.	Downregulated
AURKA	Aurora A kinase	Essential during cell mitosis in the regulation of chromosomal segregation. Upregulated in proliferating cells like cancer cells.	Downregulated
LIG4	DNA ligase 4	Necessary for the repair of double-strand DNA breaks	Downregulated
CPT2	carnitine palmitoyl transferase 2	Involved in fatty acid oxidation in the mitochondria.	Downregulated

Table S2. Gene expression. List of genes that showed significant changes between the punches extracted at 0 mm and the 10 mm punch.